STIC-ILL

From: Davis, Natalie
S nt: Monday, March 18, 2002 11:22 AM
To: STIC-ILL
Subject: 09/764918

please send the following:

1. Hammarberg, et lal., 1989, PNAS, 86(12):4367-71

Natalie A.Davis, PhD
Patent Examiner
Art Unit 1642
CM1, Rm 8B13
Mailbox 8E12
Ph (703) 308-6410

Proc. Natl. Acad. Sci. USA
Vol. 86, pp. 4367–4371, June 1989
Biochemistry

Dual affinity fusion approach and its use to express recombinant human insulin-like growth factor II

(human serum albumin binding/IgG binding)

BJÖRN HAMMARBERG*, PER-ÅKE NYGREN*, ERIK HOLMGREN†, ANETTE ELMBLAD†, MICHAEL TALLY‡, ULF HELLMAN§, TOMAS MOKS*, AND MATHIAS UHLÉN*¶

*Department of Biochemistry, Royal Institute of Technology, S-100 44 Stockholm, Sweden; †Kabigen AB, S-112 87 Stockholm, Sweden; ‡Department of Endocrinology, Karolinska Institutet, S-104 01 Stockholm, Sweden; and §Ludwig Institute for Cancer Research, Biomedical Center, S-75 123 Uppsala, Sweden

Communicated by Peter Reichard, February 28, 1989 (received for review September 27, 1988)

ABSTRACT **A dual affinity fusion concept has been developed in which the gene encoding the desired product is fused between two flanking heterologous genes encoding IgG- and albumin-binding domains. Using sequential IgG and serum albumin affinity chromatography, a full-length tripartite fusion protein is obtained. This approach was used to recover a full-length fusion product in *Escherichia coli* containing the human insulin-like growth factor II (IGF-II). Surprisingly, the recombinant IGF-II showed increased stability against proteolytic degradation in *E. coli* when produced as a dual affinity fusion protein, as compared to an N-terminal fusion protein. After site-specific cleavage of the tripartite fusion protein, IGF-II molecules with immunological and receptor binding activity were obtained without renaturation steps. The results demonstrate that proteins can fold into biologically active structures, even if provided with large flanking heterologous protein domains. The concept was further used to characterize the specific degradation of recombinant IGF-II in this heterolog us host.**

A large number of gene fusion systems to facilitate expression and purification of recombinant proteins in heterologous hosts have been described (1). Most of these expression systems have been designed for high expression levels to yield insoluble material that accumulates as aggregates in the cytoplasm (1). The disadvantage of this "inclusion body" approach is that *in vitro* refolding is required to obtain a biologically active protein. Such refolding schemes are often complex and demand specific and time-consuming optimization for each gene product.

Alternative expression systems that yield a soluble gene product with a native structure *in vivo*, therefore, have a great advantage. In particular, protein engineering studies might benefit from an approach where a biologically active protein can be obtained directly. A soluble gene product also allows the assembly of fusion proteins containing an "affinity handle" to facilitate the purification. The same general purification scheme can thus be used for a variety of gene products. For protein engineering studies this approach eliminates the need for individual purification schemes for "mutant" proteins even with altered biochemical properties (2).

However, expression in heterologous hosts of soluble gene products has been hampered by problems with proteolysis (3), in which a heterologous population of products is obtained even if an affinity-purification approach is used (4). The recovery of the full-length product from such a mixture requires additional purification steps and often gives low overall yield. This has emphasized the need for expression systems that ensure a full-length product.

In this report, we describe the development of a concept in which the gene of interest is fused between two different heterologous genes. After affinity purification of the dual affinity fusion protein by using both the N-terminal and the C-terminal domains, a full-length product is obtained, suitable for structural and functional studies. The system can also be used to facilitate molecular studies of protein degradation *in vivo* and *in vitro*, as both the C-terminal and the N-terminal regions can be recovered independently.

To develop an optimal dual affinity system, the two affinity tails should be small, soluble, and stable in various host organisms and should preferably not form dimers or multimers. It is advantageous for the tails to be secretion "competent" so that the product can be recovered from the culture medium, which facilitates the protein purification and allows the formation of disulfide bonds. Finally, it is desirable that the two affinity systems have similar binding strengths and do not cross react.

We have chosen a dual affinity fusion system based on the IgG-binding domains of staphylococcal protein A and the albumin-binding domains of streptococcal protein G. This system was used to express biologically active human insulin-like growth factor II (IGF-II) in *Escherichia coli* and also used to characterize the specific degradation of recombinant IGF-II in this heterologous host.

MATERIAL AND METHODS

Bacterial Strains and Vectors. *E. coli* HB101 (5) and RRI M15 (6) were used as hosts. Vectors used were phage M13mp18 (Pharmacia) and plasmids pEMBL8, pEMBL9 (7), pEZZ8 (8), pEZZT308 (9), pSPG2 (10), and pRIT18 (11).

DNA Constructions. DNA work was carried out as described (5). The synthesis of oligonucleotides was performed as described (12). DNA sequencing was performed as described (13).

The plasmid pRIT24 was obtained by subcloning the albumin-binding regions from streptococcal protein G derived from plasmid pSPG2. After digestion with *Eco*RI the ends were made blunt with the Klenow fragment of DNA polymerase I, a synthetic *Sal* I linker (GGTCGACC; Pharmacia) was added by ligation. Digestion with *Sal* I and *Pst* I yielded a 640-base-pair fragment that was isolated by agarose electrophoresis and inserted between the same sites in pEMBL8. The gene fragment encoding the albumin-binding domains was isolated from this plasmid by digesting with *Eco*RI and *Hin*dIII, adjacent to the insertion sites. The expression vector pEZZT308 was digested with *Eco*RI and *Hin*dIII and the fragment described above was inserted by ligation. The resulting plasmid, pRIT24, contains the staphylococcal pro-

The publication costs of this article were defrayed in part by page charge payment. This article must therefore be hereby marked "*advertisement*" in accordance with 18 U.S.C. §1734 solely to indicate this fact.

Abbreviations: HSA, human serum albumin; IGF, insulin-like growth factor; RRA, radio receptor assay.

¶To whom reprint requests should be addressed.

tein A promoter and signal sequence followed by a gene encoding a dual affinity fusion protein consisting of the ZZ region derived from staphylococcal protein A and the B1B2 region of streptococcal protein G. The IGF-II gene was assembled from synthetic oligonucleotides and inserted into the *Eco*RI and *Hin*dIII sites of pEZZ8 to yield plasmid pRIT19 (B.H., unpublished results). This plasmid was digested with *Not* I and *Msp* I and the 870-base-pair fragment containing the noncoding region upstream of the promoter, the promoter region, and the regions encoding S, ZZ, and IGF-II was isolated. This fragment was ligated with a synthetic linker (5′-CGGCGAAATCTGAAATGG and its complementary sequence, 5′-GATCCCATTTCAGATTTCGC) to change the stop codon to an ATG triplet encoding a methionine residue, which enables CNBr cleavage (see Fig. 2*B*). The linker starts with the *Msp* I site in the IGF-II gene and ends with a new *Bam*HI site in frame with the B1B2 region. The fragment was recovered by cleavage with *Eco*RI and *Bam*HI and the shorter fragment was purified and ligated with the large *Eco*RI–*Bam*HI fragment isolated from pEMBL8. After transformation to *E. coli* RR1 M15, blue colonies were isolated. DNA prepared from one of these colonies was cut with *Xho* I and *Bam*HI, cloned into M13mp18, and sequenced. The *Eco*RI–*Bam*HI fragment consisting of the mutated IGF-II gene without the stop codon was isolated and ligated to the isolated fragment from pRIT24 to yield the IGF-II dual affinity fusion plasmid, pRIT25.

Expression and Purification of Proteins. Bacteria were harvested by an osmotic shock procedure (14). The shock lysate was passed through an affinity column of human serum albumin (HSA)-Sepharose (9) or of IgG-Sepharose Fast Flow (Pharmacia) as described (15). Flow-through and fractions eluted with 0.5 M HOAc (pH 2.8) were collected and lyophilized. Eluted material was lyophilized and dissolved in PBST buffer (50 mM sodium phosphate, pH 7.1/0.9% NaCl/0.05% Tween 20) for a second affinity chromatography step or in 70% (vol/vol) formic acid for treatment with CNBr as described (4).

Pr tein Analysis. Total amount of protein was determined by spectrophotometric determination at 280 nm, using the following extinction coefficients (cm^2/mg): 0.37 for ZZ–IGF-II–B1B2, 0.17 for ZZ, 0.48 for IGF-II, and 0.45 for B1B2. The immunological activity was determined by RIA (16) and IGF-II receptor binding activity by radio receptor assay (RRA) (17). Proteins were analyzed by $NaDodSO_4$/PAGE on the Phast system (Pharmacia) and stained with Coomassie blue. Protein sequencing was performed as described by Guss *et al.* (10).

RESULTS

Dual-Affinity Concept. An outline of the basic concept is shown in Fig. 1. The gene encoding the protein of interest (X) is fused between two genes encoding two different affinity tails (A and B). In the example, the protein (X) has a protease-sensitive site. A cell lysate containing the recombinant tripartite fusion protein is first passed through an affinity column containing a tail B-specific ligand. A mixture of full-length protein and proteolytic fragments containing the C-terminal fusion protein region can thus be obtained. In a second passage through a tail A-specific affinity column, the degraded proteins flow through while full-length fusion protein is retained. After site-specific cleavage of the tails, the protein of interest (X) is obtained by passing the cleavage mixture through a mixed affinity column for tails A and B and collecting the flow-through.

The dual affinity fusion concept is attractive because it ensures recovery of full-length product and also facilitates characterization of gene products that are highly sensitive to host-specific proteases. Information about the specific degradation of recombinant proteins can be obtained by selective affinity purification. The flow-through fraction of the tail A affinity purification step yields the C-terminal degradation products (Fig. 1), which can be N-terminally sequenced. In addition, "nicked" proteins that are proteolytically cleaved but held together by disulfide bonds can be released by reduction of the material obtained by the dual affinity steps. This might provide additional information about the specific degradation sites.

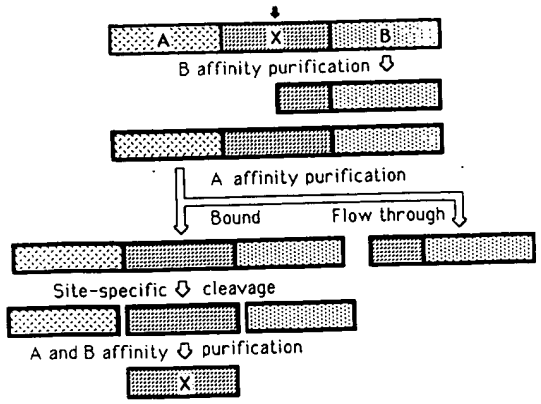

FIG. 1. Dual affinity fusion concept. The protein of interest (X) with a putative protease degradation site (solid arrow) is fused between two different affinity tails (A and B).

Dual Affinity Vector System. Nygren *et al.* (9) showed that the B1B2 fragment of the streptococcal protein G receptor binds specifically to HSA and also demonstrated that this fragment could be used to purify a fusion protein by HSA affinity chromatography. The similarities in size (≈60 amino acid residues per binding unit), binding and elution conditions, stability, and solubility make the B1B2 domain and the ZZ domain of protein A suitable fusion partners in a dual affinity system. Both receptors are monomeric and show no cross affinity between the ligands (9).

A suitable plasmid was constructed encoding the signal peptide from protein A, ZZ (a synthetic IgG-binding fragment derived from protein A), and B1B2 (an HSA-binding region of protein G). The vector pRIT24 (Fig. 2*A*) contains unique cloning sites for *Eco*RI, *Sma* I, *Bam*HI, and *Sal* I, which can be used to insert foreign genes between the two flanking gene fragments encoding the IgG- and HSA-binding domains, respectively. The promoter and signal sequence of protein A ensures efficient expression and secretion in several bacterial hosts, including *E. coli* and *Staphylococcus aureus* (18).

Mutagenesis of the Human IGF-II Gene. The gene for human IGF-II was chemically synthesized as a 240-base-pair *Eco*RI–*Hin*dIII gene fragment, encoding the mature 67-amino acid residue IGF-II (A.E., unpublished results). The synthetic gene was preceded by an ATG methionine codon and terminated in a double TAA stop codon. Using two synthetic oligonucleotides, the two stop codons were replaced by an ATG codon followed by a new *Bam*HI restriction site in the correct reading frame for the B1B2 domain (Fig. 2*A*). The nucleotide and the deduced amino acid sequences of the relevant parts of the mutated IGF-II gene are shown in Fig. 2*B*.

The gene was transferred to the pRIT24 vector using the unique *Eco*RI and *Bam*HI restriction sites. The resulting plasmid pRIT25 encodes a tripartite fusion protein with the structure schematically outlined in Fig. 2*C*. The two unique methionine residues flanking the IGF-II gene product enable site-specific cleavage with CNBr to release IGF-II. This recombinant IGF-II has a native N terminus but contains a cleavage artifact in the C terminus, either a homoserine or a homoserine lactone, depending on the pH of the buffer (19). Also shown in Fig. 2*C* is the structure of the bipartite fusion

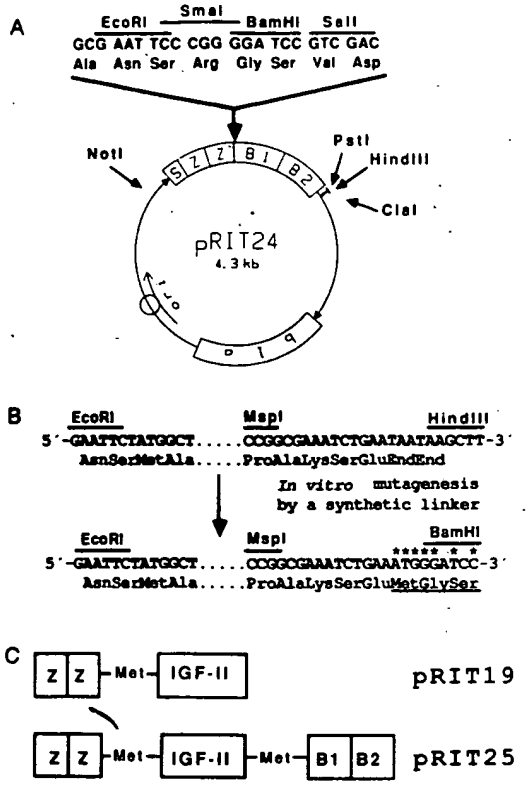

FIG. 2. Schematic drawings of the dual affinity expression vector pRIT24 (*A*), mutagenesis of the IGF-II gene (*B*), and the tripartite protein encoded by pRIT25 compared with the N-terminal fusion protein encoded by pRIT19 with its methionine residues indicated (*C*). Some relevant restriction sites are indicated. Boxes represent the genes coding for the signal sequence (S), synthetic IgG-binding region (Z), IGF-II, the HSA-binding region (B1) and (B2), and β-lactamase (bla). The origin of replication of *E. coli* is also indicated (ori) as are promoters (arrows). In *B* mutagenized bases are marked with stars.

protein between the IgG-binding ZZ domains and the human IGF-II gene (pRIT19).

Expression and Purification of the Bipartite and Tripartite Fusion Proteins. *E. coli* cells containing either plasmid pRIT19 or pRIT25 were grown overnight and the periplasmic fraction was collected by osmotic shock. Analysis by $NaDodSO_4$/PAGE (Fig. 3*A*, lane 1) shows that no or little full-length protein was obtained for the ZZ–IGF-II bipartite fusion protein, suggesting that human IGF-II is highly susceptible for proteases in *E. coli*. Surprisingly, analysis of the tripartite fusion protein (Fig. 3*B*, lane 1) demonstrates a major band corresponding to the full-length fusion protein ZZ–IGF-II–B1B2 (45 kDa), suggesting that the dual affinity fusion concept stabilizes the recombinant protein against proteolytic degradation. The lysate from the strain containing the dual affinity fusion gene (Fig. 3*B*, lane 1) was divided into two parts and passed either through an HSA column or an IgG column. Bound proteins were eluted and analyzed by electrophoresis under reducing conditions (Fig. 3*B*, lanes 2 and 3). In both cases, the full-length protein was the major product. Note that two bands of 31 and 23 kDa appeared when reduced material purified on both affinity columns was analyzed. These two bands were not observed by nonreducing $NaDodSO_4$/PAGE (data not shown) and thus suggest that nicked full-length proteins were held together by disulfide bonds.

The dual affinity approach allows comparison of degradation products purified by N-terminal or C-terminal affinity chromatography. A degradation product of 28 kDa corresponding in size to the albumin-binding domain B1B2 was

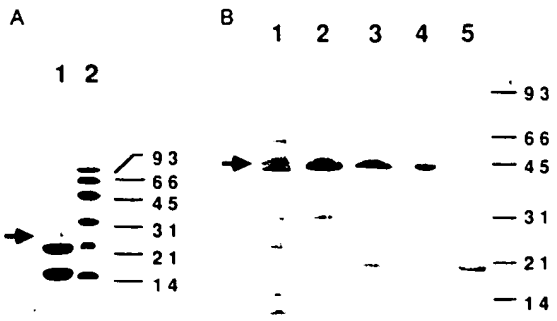

FIG. 3. Reduced $NaDodSO_4$/PAGE analysis of the bipartite (*A*) and the tripartite (*B*) fusion proteins affinity-purified from the periplasmic space of *E. coli*. (*A*) Lanes: 1, IgG affinity-purified ZZ–IGF-II (pRIT19); 2, marker proteins with sizes in kDa. (*B*) Lanes: 1, total periplasmic proteins of *E. coli* containing pRIT25; 2, HSA affinity-purified ZZ–IGF-II–B1B2 fusion protein; 3, IgG affinity-purified fusion protein; 4, IgG and HSA affinity-purified fusion protein; 5, flow-through of the HSA affinity column loaded with material affinity-purified on IgG. The positions of marker proteins are indicated with the sizes in kDa.

observed after HSA chromatography (Fig. 3*B*, lane 2), whereas a degradation product of 14 kDa corresponding to the ZZ domains was seen after IgG chromatography (Fig. 3*B*, lane 3). Thus the linker regions flanking the IGF-II moiety are susceptible to proteolysis. The material eluted from the IgG column (lane 3) was allowed to bind to an HSA column and the bound material and the flow-through were analyzed by electrophoresis (Fig. 3*B*, lanes 4 and 5, respectively). As expected the low molecular mass bands from the IgG column did not bind to the HSA column (lane 5), and a highly purified full-length protein was obtained after the two sequential affinity steps (lane 4).

Site-Specific Cleavage of the Tripartite Protein. The affinity-purified fusion protein was treated with CNBr to cleave at the two methionine residues flanking the IGF-II domain. The cleavage mixture was desalted, lyophilized, dissolved, and analyzed by IgG and/or HSA affinity chromatography and $NaDodSO_4$/PAGE (Fig. 4). The CNBr cleavage resulted in a disappearance of the full-length 45-kDa band (lane 1) and yielded new bands of 28 kDa and 14 kDa (lane 2) corresponding to the B1B2 and the ZZ domains, respectively. Only a weak band was observed corresponding to the size of the IGF-II molecule (7.5 kDa), which suggests that a large fraction of the material was lost during the desalting and lyophilization steps. This might be due to the low solubility of the recombinant IGF-II molecule without the flanking

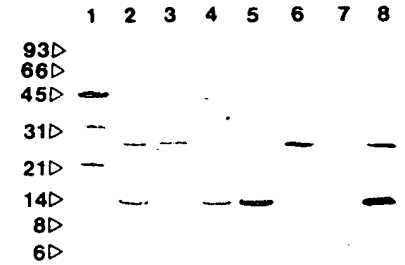

FIG. 4. $NaDodSO_4$/PAGE of cleaved tripartite fusion protein under reducing conditions. Lanes: 1, ZZ–IGF-II–B1B2 before cleavage; 2, after cleavage; 3, after cleavage flow-through of IgG column; 4, after cleavage eluate of IgG column; 5, after cleavage flow-through of HSA column; 6, after cleavage eluate of HSA column; 7, after cleavage flow-through of mixed column; 8, after cleavage eluate of mixed column. The positions of marker proteins are indicated with the sizes in kDa.

heterologous domains. The results of various affinity purification steps with cleaved material are shown in lanes 3–8 (Fig. 4). The ZZ domains were retained by the IgG column (lane 4), and the B1B2 domains were retained by the HSA column (lane 6). The mixed affinity column retained both the ZZ and B1B2 parts (lane 8), and the IGF-II molecule was recovered as flow-through (lane 7). Nonreducing NaDodSO$_4$/PAGE revealed that most material was full-length and monomeric, both before and after the site-specific cleavage (data not shown).

Immunological and Receptor-Binding Activity. The correct N terminus of the IGF-II obtained after cleavage was confirmed by N-terminal sequencing (data not shown). To show that the recombinant product was folded into a biologically active structure, despite the large heterologous flanking domains, the recombinant IGF-II (Fig. 4, lane 7) was analyzed by a RIA using chicken anti-human IGF-II antisera and by a RRA using human placental membranes. Both assays suggest a final recovery of active IGF-II molecules corresponding to ≈10 μg of IGF-II per liter of culture medium. This value was low compared to the amount of produced tripartite fusion protein, confirming the analysis of the material after cleavage and desalting by the NaDodSO$_4$/PAGE (Fig. 4, lane 2). The use of relatively hydrophobic solvents during the recovery of the cleaved material has improved the final yield of biologically active IGF-II as measured by RRA to 10–20% (data not shown). The parallel curves in Fig. 5 *A* and *B* (RIA and RRA, respectively) show that native and recombinant IGF-II compete with similar or identical affinity with labeled native IGF-II. In addition, the specific RRA activity of the recombinant IGF-II obtained after a single purification by ion-exchange chromatography is approximately the same as purified native IGF-II obtained from human serum (data not shown). The results, therefore, demonstrate that the dual affinity fusion approach yields active peptide hormone without any renaturation schemes.

Analysis of the Protease-Sensitive Site of IGF-II in *E. coli*. Recombinant IGF-II has one or several protease-sensitive sites recognized by a host-specific protease in *E. coli* (B.H., unpublished results). The tripartite fusion protein obtained from *E. coli* can, therefore, be used to characterize the degradation products. Reduction of the disulfide bonds in the affinity-purified fusion protein yields two smaller degradation products (Fig. 3*B*, lane 4) that correspond to the two parts of a nicked tripartite molecule. The full-length fusion protein purified by both IgG and HSA chromatography was, therefore, reduced by 250 mM 2-mercaptoethanol to break all disulfide bonds. The reduced material was separated by size-exclusion chromatography under reducing conditions (Fig. 6*A*) into three major peaks corresponding to ≈45 kDa (I), ≈30 kDa (II), and ≈20 kDa (III). The protein material from these peaks was recovered and the N-terminal sequences were determined by Edman degradation. The results (Fig. 6A) revealed that peaks I and III contained the expected N terminus of the tripartite protein, and peak II yielded a sequence starting with Arg-38 or Ser-39 of the native IGF-II. The proteolytic cleavage occurred in ≈75% of the product between the Arg-37 and the Arg-38, and 25% was cleaved between the Arg-38 and the Ser-39.

The sequences and the sizes of the various peptides suggest a proteolytic site in the IGF-II moiety that yields degradation products II and III (Fig. 6*B*). The fact that these degradation products are obtained after reduction of a dual-affinity-purified material suggests that they correspond to the two parts of a nicked molecule held together by disulfide bridges.

DISCUSSION

The present investigation shows that the dual affinity fusion approach can be used to produce biologically active human IGF-II in *E. coli* without a complex renaturation scheme. The results demonstrate that this peptide hormone, containing

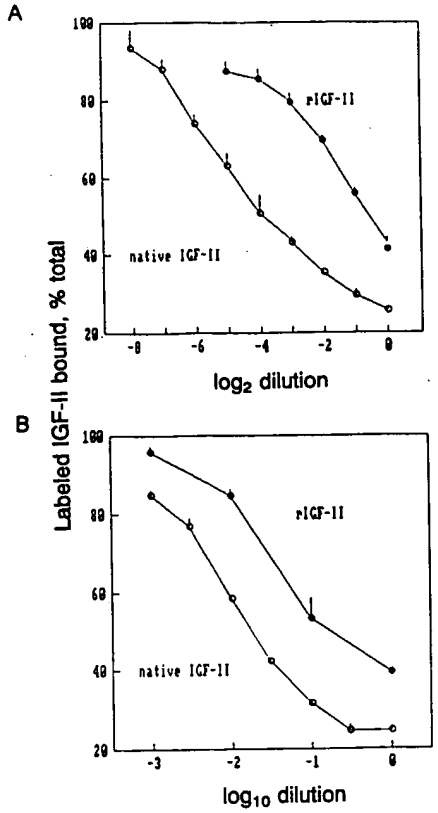

FIG. 5. Analysis of IGF-II for immunological and receptor binding activity using RIA (*A*) and RRA (*B*). Crude lyophilized recombinant IGF-II was reconstituted in 50 mM NH_4OAc (pH 7.4) and added in 1:2 (RIA) and 1:10 (RRA) dilution steps with material corresponding to 1 μg (*A*) and 10 μg (*B*) of cleaved fusion protein as the initial sample (dilution step 0). Native IGF-II purified from human serum was used as standard and the initial sample (dilution step 0) consisted of 10 ng (RIA) and 100 ng (RRA) of purified native IGF-II, respectively. The standard deviations for various triplicate determinations are shown as bars. ●, Recombinant IGF-II; ○, native IGF-II.

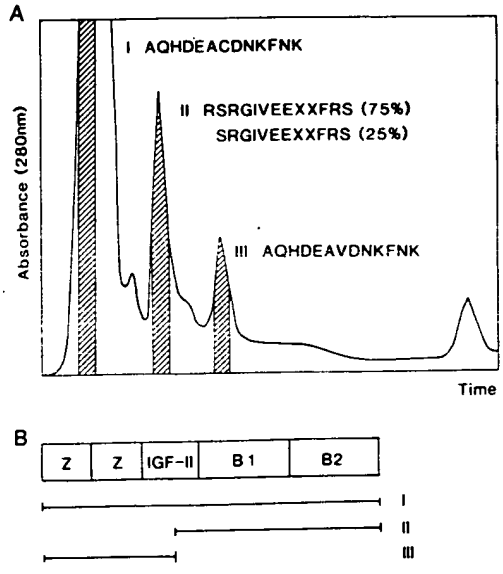

FIG. 6. (*A*) Chromatogram of gel filtration of reduced full-length tripartite protein. The N-terminal sequences of corresponding peaks are indicated using the single-letter amino acid code. (*B*) Peptides resulting from proteolytic degradation.

three disulfide bonds, can fold into a biologically active structure, even when flanked by relatively large affinity domains in both the C- and N-terminal ends. The produced fusion protein has four parts, (*i*) a signal sequence from staphylococcal protein A, (*ii*) an IgG-binding region of synthetic origin, (*iii*) the human IGF-II, and (*iv*) an albumin-binding region from streptococcal protein G. The fact that all of these parts of the fusion protein are functional demonstrates the remarkable tolerance of recombinant fusion proteins to fold as long as the individual domains of the peptides are intact.

Expression of recombinant IGF-II in *E. coli* using N-terminal fusion to the IgG-binding domain yielded a highly degraded product (Fig. 3*A*, lane 1). In contrast, the dual affinity approach yielded a mostly full-length tripartite fusion protein (Fig. 3*B*), and biological activity was obtained after site-specific cleavage (Fig. 5). This interesting and surprising result suggests that the C-terminal affinity domain stabilizes IGF-II.

Native human IGF-II *in vivo* is produced with a C-terminal extension of 21 amino acid residues called region E (20). The function of this region is still unknown, but it is tempting to speculate that its role is to stabilize the newly synthesized IGF-II molecule from proteolysis or to facilitate folding in the correct tertiary structure. The question arises whether the C-terminal affinity domain is able to contribute some of the functions of the native region E. This may be accomplished by sterical protection, by protein interactions involving the acidic protein G domain, or by influencing the secretion mechanism during the membrane translocation.

The analysis of the break-down products revealed that the protease responsible for the major degradation of human IGF-II in *E. coli* is probably an endoprotease with a specificity for basic amino acids (Fig. 6). Interestingly, the N-terminal sequencing revealed that most of the material was nicked after the two arginine residues at position 37 and 38 of mature IGF-II, but some molecules were nicked between these two arginines. The presumptive protease may, therefore, have a trypsin-like activity with a preference to cleave after one or two basic residues. These results have prompted us to investigate if the outer membrane protease OmpT, with a specificity for basic residues (3), might be responsible for the degradation. The fusion protein ZZ-IGF-II encoded by pRIT19 (Fig. 2*C*) is highly susceptible to degradation in a wild-type *E. coli* strain (Fig. 3*A*, lane 1). In contrast, >80% of the material was found to be full-length when produced in an *ompT* mutant strain (B.H., unpublished results), suggesting that the proteolytic instability of recombinant IGF-II in *E. coli* is indeed caused by the OmpT protease. This demonstrates the importance of molecular tools, such as the dual affinity approach, to study and characterize protease degradation of recombinant proteins.

It is noteworthy that human IGF-I can be efficiently expressed in *E. coli* without severe proteolysis using the protein A system (15). A comparison of the primary amino acid sequences of the structurally similar IGF-I and -II reveals that the two arginines recognized by a protease in *E. coli* are present on both molecules. The fact that IGF-I molecules are relatively insensitive to proteolysis, therefore, suggests that these regions are structurally different or follow different folding pathways that influence their protease susceptibility.

There are a number of reasons to use this dual affinity fusion concept. Many applications involving heterologous expression of recombinant proteins require a defined and homogenous material for immunizations, diagnostics, or protein characterization. Although the dual affinity approach also yields nicked proteins, the system ensures that only the full-length product is recovered. Another important application, already discussed, is the study of proteolysis both *in vivo* or *in vitro*. The protein can be purified using the N- or the C-terminal region or both regions and can subsequently be characterized by protein sequencing and analysis. The protocol used in this paper, which involves purification of the full-length protein by two affinity steps followed by reduction of disulfide bonds, affinity purification of the C-terminal end, and then N-terminal sequencing of the obtained fragment, can be used to gain information about the proteolysis site in any inserted protein.

The dual affinity concept can also be used to answer biological questions of more general nature. Experiments to characterize error frequencies of ribosomes have been designed using this approach (L. Isaksson and M.U., unpublished results). The low solubility of recombinant human IGF-II (21) further accentuates the advantage of producing heterologous proteins with soluble fusion partners. The fusion protein can be recovered and purified from the cell lysate in a soluble form. In conclusion, the dual affinity fusion concept provides a general and simple tool to study translational and posttranslation modifications and facilitates the expression of recombinant proteins with low solubility.

We are grateful to Drs. Björn Nilsson, Lennart Philipson, Maris Hartmanis, Staffan Josephson, and Lars Abrahmsén for critical comments and advice. This investigation was supported by grants from the Swedish Board of Technical Development, by the Swedish Natural Research Council, and by the Swedish Medical Research Council (Grants 6897 and 4224).

1. Marston, F. A. O. (1986) *Biochem. J.* **240**, 1–12.
2. Carter, P. & Wells, J. A. (1987) *Science* **237**, 394–399.
3. Grodberg, J. & Dunn, J. J. (1988) *J. Bacteriol.* **170**, 1245–1253.
4. Olsson, H., Lind, P., Pohl, G., Henrichson, C., Mutt, V., Jörnvall, H., Josephson, S., Uhlén, M. & Lake, M. (1988) *Peptides* **9**, 301–307.
5. Maniatis, T., Fritsch, E. F. & Sambrook, J. (1982) *Molecular Cloning: A Laboratory Manual* (Cold Spring Harbor Lab., Cold Spring Harbor, NY).
6. Langley, K. E., Villarejo, M. R., Fowler, A. V., Zamenhof, P. J. & Zabin, I. (1975) *Proc. Natl. Acad. Sci. USA* **72**, 1254–1257.
7. Dente, L., Cesareni, G. & Cortese, R. (1983) *Nucleic Acids Res.* **11**, 1645–1655.
8. Löwenadler, B., Jansson, B., Paleus, S., Holmgren, E., Nilsson, B., Moks, T., Palm, G., Josephson, S., Philipson, L. & Uhlén, M. (1987) *Gene* **58**, 87–97.
9. Nygren, P.-Å., Eliasson, M., Palmcrantz, E., Abrahmsén, L. & Uhlén, M. (1988) *J. Mol. Recognition* **1**, 69–74.
10. Guss, B., Eliasson, M., Olsson, A., Uhlén, M., Frej, A.-K., Jörnvall, H., Flock, J.-I. & Lindberg, M. (1986) *EMBO J.* **5**, 1567–1575.
11. Elmblad, A., Josephson, S. & Palm, G. (1982) *Nucleic Acids Res.* **10**, 3291–3301.
12. Moks, T., Abrahmsén, L., Holmgren, E., Billich, M., Olson, A., Uhlén, M., Pohl, G., Sterky, C., Hultberg, H., Josephson, S., Holmgren, A., Jörnvall, H. & Nilsson, B. (1987) *Biochemistry* **26**, 5239–5244.
13. Olsson, A. & Uhlén, M. (1986) *Gene* **45**, 175–181.
14. Nossal, N. G. & Heppel, L. A. (1966) *J. Biol. Chem.* **241**, 3055–3062.
15. Moks, T., Abrahmsén, L., Österlöf, B., Josephson, S., Östling, M., Enfors, S.-O., Persson, I., Nilsson, B. & Uhlén, M. (1987) *Bio/Technology* **5**, 379–382.
16. Enberg, G. & Hall, K. (1984) *Acta Endocrinol. (Copenhagen)* **107**, 164–170.
17. Takano, K., Hall, K., Ritzén, M., Iselius, L. & Sivertsson, H. (1976) *Acta Endocrinol. (Copenhagen)* **82**, 449–459.
18. Abrahmsén, L., Moks, T., Nilsson, B., Hellman, U. & Uhlén, M. (1985) *EMBO J.* **4**, 3901–3906.
19. Gross, E. (1967) *Methods Enzymol.* **11**, 238–255.
20. Zumstein, P. P., Lüthi, C. & Humbel, R. E. (1985) *Proc. Natl. Acad. Sci. USA* **82**, 3169–3172.
21. Furman, T. C., Epp, J., Hsiung, H. M., Hoskins, J., Long, G. L., Medelsohn, L. G., Schoner, B., Smith, D. P. & Smith, M. C. (1987) *Bio/Technology* **5**, 1047–1051.

09/764,918

Your SELECT statement is:
s cysteine(w)loop and insert?

Items	File
1	5: Biosis Previews(R)_1969-2002/Dec W1
3	98: General Sci Abs/Full-Text_1984-2002/Oct
2	149: TGG Health&Wellness DB(SM)_1976-2002/Nov W4
1	442: AMA Journals_1982-2002/Dec B3

SYSTEM:OS - DIALOG OneSearch
File 5:Biosis Previews(R) 1969-2002/Dec W1
(c) 2002 BIOSIS
***File 5: Alert feature enhanced for multiple files, duplicates** removal, customized scheduling. See HELP ALERT.
File 98:General Sci Abs/Full-Text 1984-2002/Oct
(c) 2002 The HW Wilson Co.
File 442:AMA Journals 1982-2002/Dec B3
(c)2002 Amer Med Assn -FARS/DARS applyYour SELECT statement is:
s (chimer? or fusion or heterolo?) and cysteine(w)loop

Items	File
3	5: Biosis Previews(R)_1969-2002/Dec W1
6	34: SciSearch(R) Cited Ref Sci_1990-2002/Dec W2
1	71: ELSEVIER BIOBASE_1994-2002/Dec W1
3	73: EMBASE_1974-2002/Dec W1
3	98: General Sci Abs/Full-Text_1984-2002/Oct
1	144: Pascal_1973-2002/Dec W2
2	149: TGG Health&Wellness DB(SM)_1976-2002/Nov W4
5	155: MEDLINE(R)_1966-2002/Nov W3
2	156: ToxFile_1965-2002/Nov W3

SYSTEM:OS - DIALOG OneSearch
File 5:Biosis Previews(R) 1969-2002/Dec W1
(c) 2002 BIOSIS
***File 5: Alert feature enhanced for multiple files, duplicates** removal, customized scheduling. See HELP ALERT.
File 155:MEDLINE(R) 1966-2002/Nov W3
***File 155: For updating information please see Help News155. Alert** feature enhanced with customized scheduling. See HELP ALERT.
File 34:SciSearch(R) Cited Ref Sci 1990-2002/Dec W2
(c) 2002 Inst for Sci Info
***File 34: Alert feature enhanced for multiple files, duplicates** removal, customized scheduling. See HELP ALERT.

Set	Items	Description
S1	437637	HETEROL? OR CHIMER? OR FUSION
S2	18	S1 AND CYSTEINE(W)LOOP?
S3	11	RD (unique items)

3/9/3 (Item 3 from file: 5)
DIALOG(R)File 5:Biosis Previews(R)
(c) 2002 BIOSIS. All rts. reserv.

10063616 BIOSIS NO.: 199598518534
An infectious chimeric **human immunodeficiency virus type 2 (HIV-2) expressing the HIV-1 principal neutralizing determinant.**
AUTHOR: Mamounas Michael; Looney David J(a); Talbott Randy; Wong-Staal Flossie
AUTHOR ADDRESS: (a)Infectious Dis. 9-111F, San Diego Dep. Veteran's Affairs Med. Cent., 3350 La Jolla Village Drive**USA
JOURNAL: Journal of Virology 69 (10):p6424-6429 1995
ISSN: 0022-538X
DOCUMENT TYPE: Article
RECORD TYPE: Abstract
LANGUAGE: English

ABSTRACT: The human immunodeficiency virus type 1 strain MN (HIV-1-MN) principal neutralizing determinant (PND, V3 loop) was introduced into infectious molecular clones HIV-2-KR and simian immunodeficiency virus mm239 (SIV-mm239) by hybridization PCR, replacing the corresponding HIV-2

or SIV envelope **cysteine loops** with the HIV-1 coding sequence. The HIV-2 **chimera** (HIV-2-KR-MNV3) was found to be capable of infecting a number of T-cell lymphoblastic cell lines as well as primary peripheral blood mononuclear cells. In contrast, the SIV **chimera** (SIV-239MNV3) was not replication competent. Envelope produced by HIV-2-KR-MNV3 but not the parental HIV-2-KR was recognized by V3-specific and HIV-1-specific polyclonal antisera in radioimmunoprecipitation assays. HIV-2-specific antisera recognized both the **chimeric** and parental virus but not HIV-1-MN. The **chimeric** HIV-2-KR-MNV3 virus proved to be exquisitely susceptible to neutralization by HIV-1-specific and V3-specific antisera, suggesting the potential for use in animal models designed to test HIV-1 vaccine candidates which target the PND.

REGISTRY NUMBERS: 52-90-4: CYSTEINE; 164185-85-7: GENBANK-U22047; 160119-73-3: GENBANK-U17449

DESCRIPTORS:

MAJOR CONCEPTS: Biochemistry and Molecular Biophysics; Blood and Lymphatics (Transport and Circulation); Genetics; Immune System (Chemical Coordination and Homeostasis); Infection; Metabolism; Microbiology; Pharmacology

BIOSYSTEMATIC NAMES: Cercopithecidae--Primates, Mammalia, Vertebrata, Chordata, Animalia; Pongidae--Primates, Mammalia, Vertebrata, Chordata, Animalia; Retroviridae--Viruses

ORGANISMS: chimpanzee (Pongidae); macaque (Cercopithecidae); simian immunodeficiency virus (Retroviridae)

BIOSYSTEMATIC CLASSIFICATION (SUPER TAXA): animals; chordates; mammals; microorganisms; nonhuman mammals; nonhuman primates; nonhuman vertebrates; primates; vertebrates; viruses

CHEMICALS & BIOCHEMICALS: CYSTEINE; GENBANK-U22047; GENBANK-U17449

MOLECULAR SEQUENCE DATABANK NUMBER: molecular sequence data; nucleotide sequence; GENBANK-U17449; GENBANK-U22047

MISCELLANEOUS TERMS: ANIMAL MODELS; ENVELOPE **CYSTEINE LOOPS** ; HUMAN IMMUNODEFICIENCY VIRUS TYPE 1 VACCINE CANDIDATES; V3 LOOP

JOURNAL OF VIROLOGY, Oct. 1995, p. 6424–6429
0022-538X/95/$04.00+0

Vol. 69, No. 10

An Infectious Chimeric Human Immunodeficiency Virus Type 2 (HIV-2) Expressing the HIV-1 Principal Neutralizing Determinant

MICHAEL MAMOUNAS,[1] DAVID J. LOONEY,[2]* RANDY TALBOTT,[1]†
AND FLOSSIE WONG-STAAL[1]

Departments of Medicine and Biology, University of California, San Diego, La Jolla, California 92093-0665,[1] and Infectious Diseases, Department of Veteran's Affairs Medical Center, San Diego, California 92161[2]

Received 24 March 1995/Accepted 3 July 1995

The human immunodeficiency virus type 1 strain MN ($HIV\text{-}1_{MN}$) principal neutralizing determinant (PND, V3 loop) was introduced into infectious molecular clones $HIV\text{-}2_{KR}$ and simian immunodeficiency virus mm239 (SIV_{mm239}) by hybridization PCR, replacing the corresponding HIV-2 or SIV envelope cysteine loops with the HIV-1 coding sequence. The HIV-2 chimera ($HIV\text{-}2_{KR\text{-}MNV3}$) was found to be capable of infecting a number of T-cell lymphoblastic cell lines as well as primary peripheral blood mononuclear cells. In contrast, the SIV chimera ($SIV_{239MNV3}$) was not replication competent. Envelope produced by $HIV\text{-}2_{KR\text{-}MNV3}$ but not the parental $HIV\text{-}2_{KR}$ was recognized by V3-specific and HIV-1-specific polyclonal antisera in radioimmunoprecipitation assays. HIV-2-specific antisera recognized both the chimeric and parental virus but not $HIV\text{-}1_{MN}$. The chimeric $HIV\text{-}2_{KR\text{-}MNV3}$ virus proved to be exquisitely susceptible to neutralization by HIV-1-specific and V3-specific antisera, suggesting the potential for use in animal models designed to test HIV-1 vaccine candidates which target the PND.

One obstacle in the development of vaccines against human immunodeficiency virus type 1 (HIV-1) infection has been the lack of animal models suitable for rapid, statistically meaningful, and inexpensive testing. Infection of a variety of nonhuman primates with HIV-1 has been reported, including chimpanzees (*Pan troglodytes*) (2), gibbons (*Hylobates lar*) (20), and macaques (*Macaca nemestrina*) (1, 8). Unfortunately, the former two species are both endangered and expensive, all but prohibiting conclusive studies. Macaques are more readily available and much less expensive than chimpanzees or gibbons; however, models of HIV-1 infection of *M. nemestrina* are still being evaluated, and some investigators have observed only limited replication of HIV-1 in pigtailed macaques even after administration of large inocula (23), raising concerns about sensitivity. Because simian immunodeficiency virus (SIV), such as SIV_{mac239}, readily infects macaques (9, 16, 18) and produces disease resembling human AIDS, chimeras between SIV_{mac} and HIV-1 (SHIV) which contain the HIV-1 *env* and/or *nef* gene have been explored as a means of generating viruses which are both capable of infecting macaques (cynomolgus species) and yet susceptible to immune responses elicited by HIV-1-based vaccine candidates. Multiple HIV-2 strains have also been shown to be infectious in macaques (3, 5, 7, 23, 26) and, more recently, in baboons (5).

The V3 loop of the HIV-1 envelope continues to be an attractive target for epitope-based vaccines, including those currently being evaluated in phase I human trials. In chimpanzee models, neutralizing V3 antibodies are sufficient to protect against homologous challenge virus (6), and V3 antibodies and V3-based peptide vaccines have been shown to elicit broadly neutralizing antibodies against primary isolates (10, 33, 36) in small animals. Similarly, antisera to HIV-2 V3 peptides have been shown to neutralize HIV-2 viruses in a type-specific fashion (4), as observed (24) for HIV-1. In contrast, SIV V3 loop peptides do not appear to elicit neutralizing antibodies (13). An inspection of available aligned sequences (22) reveals that the V3 loops of sequenced HIV-2 viruses are variable, though less extensively than HIV-1 (~12 to 18% divergent for HIV-2, compared with 14 to 40% for HIV-1). In contrast, SIV sequences are highly conserved in this region, suggesting that the V3 loop of HIV-2 but not SIV may face selective pressures similar to those faced by the V3 loop of HIV-1 in vivo. To facilitate the development of an inexpensive nonhuman primate model for testing the ability of HIV-1 vaccine candidates targeting the V3 region to block infectivity, the creation of a chimera in which the HIV-2 V3 loop is replaced with that of HIV-1 appears to be technically feasible and consistent with the biology of these viruses.

By using the infectious $HIV\text{-}2_{KR}$ molecular clone (17) and the SIV_{mm239} molecular clone (28), $HIV\text{-}1_{MN}$ V3 loop chimeras were constructed by hybridization PCR. The HIV-2 chimera ($HIV\text{-}2_{KR\text{-}MNV3}$) proved to be replication competent in a number of T-cell lines and primary lymphocytes. In contrast, the SIV/HIV-1 V3 chimera was not replication competent in vitro, strengthening the suggestion that the role of the V3 region and/or tolerance for variability differs significantly between SIV and HIV-1 or HIV-2. The chimeric HIV-2 envelope was recognized by antibodies against $HIV\text{-}1_{MN}$ V3 peptides and native envelope. In addition, the $HIV\text{-}2_{KR\text{-}MNV3}$ recombinant virus was efficiently neutralized by HIV-1 V3-specific antisera, further suggesting retention of a similar conformation and biological function in this construct and potential utility in vaccine models.

* Corresponding author. Mailing address: Infectious Diseases 9-111F, San Diego Department of Veteran's Affairs Medical Center, 3350 La Jolla Village Dr., San Diego, CA 92161. Phone: (619) 552-8585, ext. 2626. Fax: (619) 534-7957. Electronic mail address: dlooney@ucsd.edu.

† Present address: Pharmaceutical Research Division, Department of Oncology, Bristol-Meyers-Squibb, Princeton, NJ 08543-5303.

MATERIALS AND METHODS

RIPA. For the radioimmunoprecipitation assay (RIPA), Molt 4/8 cells ($\sim 10^7$) acutely infected with HIV-2_{KR}, HIV-$2_{KR\text{-}MNV3}$, or HIV-1_{MN} were starved for 2 h in cysteine- and methionine-free RPMI medium supplemented with 5% dialyzed fetal calf serum. The cells were then metabolically labeled with 200 μCi each of [^{35}S]cysteine and [^{35}S]methionine per ml for 6 h and then lysed in 4 ml of RIPA buffer (50 mM Tris-HCl [pH 7.2], 150 mM NaCl, 0.1% sodium dodecyl sulfate [SDS], 1% Triton X-100, 1% sodium deoxycholate, 1 mM phenylmethylsulfonyl fluoride, adjusted to pH 7.8) at 4°C for 30 min. Lysates were cleared by 20,000 × *g* centrifugation in a 50 Ti rotor for 1 h. Sera used for immunoprecipitation included human serum from an HIV-1-infected AIDS patient, serum from a macaque infected with HIV-2_{KR} and HIV-2_{287} (21), and normal human sera. Sera were diluted 1:100 in phosphate-buffered saline (PBS) and incubated with washed Sepharose-protein A. From 5×10^6 to 10×10^6 Bq of each labelled lysate per reaction was then added after washing. After they were washed four times, precipitates were electrophoresed on a 9% polyacrylamide–SDS gel and visualized by autoradiography.

Mutagenesis. Starting plasmids included bipartite plasmids containing the 5′ (pKTM) and 3′ (pRTsac) portions of the HIV-2_{KR} provirus (32) and plasmids p239SPE and p239SPSP (gift of R. C. Desrosiers), containing the 5′ and 3′ portions of the SIV_{mm239} provirus, respectively (28). Mutagenesis was performed by hybridization PCR (34) (see Fig. 1) with central primers of 82 and 85 nucleotides covering 159 bp encoding the entire 99-bp HIV-1_{MN} principal neutralizing determinant (PND) and flanking HIV-2_{KR} sequences, overlapping in the central 23 nucleotides. For HIV-2_{KR}, the inner primers used were (5′ fragment, downstream primer at 7798) 5′-GCT-TTC-TTC-CAA-ATC-ACC-TCC-GAA-CCA-ACA-TGT-GCT-TGG-TCT-TAT-AGT-TCC-TAT-TAT-ATT-TTT-TGT-TGT-ATA-AAA-TGC-TGT-CCC-TGG-TCC-T-3′ and (3′ fragment, upstream primer at 7652) 5′-GCT-TAA-AAT-ACA-CAT-TAT-AAT-CTC-ACA-ATG-CAT-TGT-ACA-AGA-CCC-AAC-TAC-AAT-AAA-AGA-AAA-AGG-ATA-GGA-CCA-GGG-ACA-GCA-TTT-TAT-A-3′. Outside primers used were in *vpr* (upstream 5′ fragment at 6329) 5′-ATG-ACT-GAA-GCA-CCA-GCA-GAG-TTT-3′ and in *nef* (downstream, 3′ fragment, 9948) 5′-CAA-GAG-GGA-TAC-CAT-TTA-GTT-AA-3′. The 3.6-kb PCR product contained a 1.2-kb *Spe*I-*Eco*NI fragment (6836 to 8094) which was cloned back into pRTsac deleted of the corresponding *Spe*I-*Eco*NI region to generate plasmid pRT-MNV3, containing the 3′ portion of chimeric virus KR-MNV3.

An essentially identical procedure was used to substitute the HIV-1 MN V3 loop into SIV_{mac239} with 79- and 90-bp primers. The inside primers used were (5′ fragment, downstream at 7892) 5′-CCT-TCC-ATT-TTC-CTC-CAA-ACC-AAC-AAT-GTG-CTT-GTC-TTA-TAG-TTC-CTA-TTA-TAT-TTT-TTG-TTG-TAT-AAA-ATG-CTC-TCC-C-3′ and (3′ fragment, upstream 7251) 5′-GTA-TTA-TAA-TCT-AAC-AAT-GAA-ATG-TAC-AAG-ACC-CAA-CTA-CAT-ATA-GGA-CCA-GGG-AGA-GCA-TTT-TAT-ACA-AC-3′. Outside primers used were in *env* (5′ upstream primer at 7768) 5′-CAT-CAA-CAA-CAT-CAA-CGA-CAG- C-3′ and (3′ downstream primer at 8382) 5′-CCC-CCA-CAG-ATG-TGA-AGA-GGT-A-3′. The 1.1-kb PCR product contained a 1.0-kb *Spe*I-*Cla*I fragment (7301 to 8329) which was cloned back into p239SPE3′ deleted of the corresponding region to create p239SP-MNV3, containing the 3′ portion of the chimeric 239MNV3 virus.

Transfection. Proviral DNA for transfection was produced by cutting pKTM and pRT-MNV3 or p239SPSP and p239SP-MNV3 with *Sac*I, followed by centrifugation through a Millipore Ultrafree-Probind column to remove the restriction enzyme, and ligation with T4 DNA ligase in a total volume of 250 μl. Molt 4/8 cells were washed with RPMI 1640 medium containing 10% fetal bovine serum, and cells were resuspended at a density of 4×10^5/ml. Cells (400 μl) were mixed with 4 μg of ligated DNA and electroporated at 250 V at 500 μF with an electroporation apparatus. The cells were then resuspended in a total volume of 10 ml in RPMI 1640 medium with 10% fetal bovine serum and incubated at 37°C, 5% CO_2, 95% humidity. Samples were taken periodically and assayed for p26 production with a Coulter SIV p26 antigen capture kit (32).

Titration of virus stocks. Tenfold serial dilutions in 100-μl volumes were made in 96-well U-bottomed plates in quadruplicate with virus stocks expanded in Molt 4/8 cells after initial transfection and concentrated 200-fold by ultracentrifugation. The diluted virus was then incubated with 4×10^4 Molt 4/8 cells per well in a total volume of 200 μl in 96-well microtiter plates. After 5 to 7 days, the number of syncytia in each well was scored, and the virus titer was determined by the method of Reed and Muench (27).

Neutralization assay. Serum samples were diluted 1:4 in microtiter plates in quadruplicate and then incubated with 100 50% tissue culture infectious doses ($TCID_{50}$) of virus at 4°C for 45 min and then at 20°C for 20 min in a total volume of 60 μl. Molt 4/8 cells were then added to each well at a density of 4×10^4 cells per well in a total volume of 100 μl, and plates were incubated at 37°C for 3 h. Wells were then fed with fresh RPMI medium to a total of 200 μl per well. After 5 to 7 days, syncytia were scored, and the reduction in viral infectivity produced by each serum was determined. Values of neutralization are expressed as the reciprocal of the dilution necessary to give a ≥90% reduction in syncytium formation. The sera used included those used for radioimmunoprecipitation as well as a variety of monospecific polyclonal peptide antisera (including G19-9 and G18-9 MN V3 antisera, courtesy of Thomas Palker [25], and GP-06 and GP-16 antisera, courtesy C.-Y. Wang United Biomedical Inc. [33]).

Isolation of genomic DNA for sequencing. Infected and uninfected cells (5×10^6 to 10×10^6) were collected by centrifugation and washed once with Hanks' balanced salt solution. Pellets were resuspended in 0.25 ml of PBS and 2.25 ml of TE to which 0.25 ml of 10% SDS was added. After gentle mixing, 50 μl of proteinase K (10 mg/ml) was added. Lysates were then incubated at 37°C for 4 h to overnight. Subsequently, 1.2 ml of 5 M NaCl was added, the mixtures were vortexed, and precipitate was removed by centrifugation at 900 × *g* for 15 min. To precipitate DNA, 7.5 ml of ice-cold ethanol was added to the supernatants. DNA was then spun onto a glass rod, washed once with 70% ethanol, and then redissolved in TE.

Regions containing V3 loop and flanking sequences were then amplified from cellular genomic DNA with primers (upstream) 5′-GGT-TTA-GAT-ACT-GTG-CAC-CAC-C-3′ and (downstream) 5′-CCC-CTC-CTG-AGG-ATT-GAT-TAA-AGA-CTA-3′. These primers amplify the entire 105 bp of the V3 loop, 245 bp of flanking sequences on the 5′ side of the V3, and 179 bp of flanking sequences on the 3′ side of the V3. PCR was performed in a total volume of 100 μl with 1 μg of genomic DNA, 10 mM Tris-HCl (pH 8.3), 50 mM KCl, 5 mM $MgCl_2$, each deoxynucleoside triphosphate at 0.2 mM, 100 pmol of each primer, and 1.0 U of *Taq* DNA polymerase (Promega). Amplification was carried out for 35 cycles at 1 min at 94°C, 1 min at 55°C, and 2 min at 72°C.

After visualization of PCR samples by agarose gel electrophoresis, the amplified fragments were diluted 1:100 and then cloned directly into a plasmid vector with a T/A cloning kit from Invitrogen. Following transformation of the ligation mixture, 10 colonies were selected at random for sequencing.

DNA sequencing. DNA sequencing was performed by the chain termination method on double-stranded plasmid DNA with a Bio-Rad Bst DNA sequencing kit and [α-^{35}S]dATP.

Tissue culture. T-cell lines Molt 3, Molt 4/8, SupT1, H9, Jurkat, MT2, and MT4 and the monocytoid line U937 were maintained in RPMI 1640 (GIBCO Laboratories, Grand Island, N.Y.) supplemented with 10% fetal calf serum, 2 mM L-glutamine, and 100 U of penicillin and 100 μg of streptomycin per ml in a humid atmosphere at 37°C in the presence of 5% CO_2.

Peripheral blood mononuclear cells (PBMC) were isolated from 15 ml of whole blood (human or macaque) with Ficoll-Paque (Pharmacia) and resuspended in the above-mentioned growth medium supplemented with 5 μg of phytohemagglutinin (PHA-P; Pharmacia) per ml. Following 48 to 72 h of stimulation, the cells were washed and infected as described below. After infection, PBMC were supplemented with 100 U of recombinant human interleukin-2 (IL-2; Genzyme) per ml, and the medium was replaced every 3 days.

Infectivity assays. For experiments to determine the cell tropism of the chimeric virus KR-MNV3, T-cell lines Molt 3, SupT1, H9, Molt 4/8, Jurkat, MT2, and MT4 and the monocytoid cell line U937 were incubated overnight at a multiplicity of infection (MOI) of 0.01 $TCID_{50}$/cell with either KR or KR-MNV3. Human PBMC stimulated with PHA-P (5 μg/ml) were inoculated with 0.1 $TCID_{50}$/cell with constant mixing at 37°C over 3 h. The cells were then washed three times with Hanks' balanced salt solution and incubated at 37°C. At intervals, samples were taken and stored at −20°C for p26 analysis with an SIV antigen capture kit.

GenBank accession numbers. The complete nucleotide sequence of HIV-2_{KR} is available under GenBank accession number U22047. The complete nucleotide sequence of SIV_{mac239} is available under GenBank accession numbers M33262 and M61062 to M61093. The complete nucleotide sequence of HIV-1_{MN} is available under GenBank accession number M17449.

RESULTS

Construction of chimeric viruses. The HIV-1_{MN} V3 loop was substituted for the HIV-2_{KR} V3 loop and the SIV_{mm239} V3 loop by two-step hybridization PCR (Fig. 1; see Materials and Methods). The substitutions were designed so that only sequences between the two cysteine residues flanking the V3 region were altered. The HIV-1_{MN} V3 loop sequence was chosen for creation of chimeras because the MN V3 closely matches the North American consensus sequence for V3 loops and is represented in the majority of V3-based peptide vaccines (and envelope-based vaccines) that are currently being tested. Following mutagenesis and subcloning, the sequences of the chimeric clones were verified by sequencing plasmid DNA in the region spanning the V3 loop as well as the flanking sequences amplified by PCR during construction. The chimeric viruses were designated KR-MNV3 and SIV-MNV3, respectively.

Growth of chimeric viruses. After ligation, KR-MNV3 and SIV-MNV3 were transfected into T-cell lines highly permissive for replication (Molt 4/8, highly permissive for HIV-1 and HIV-2, and CEMX174 and C8166 cells, highly permissive for

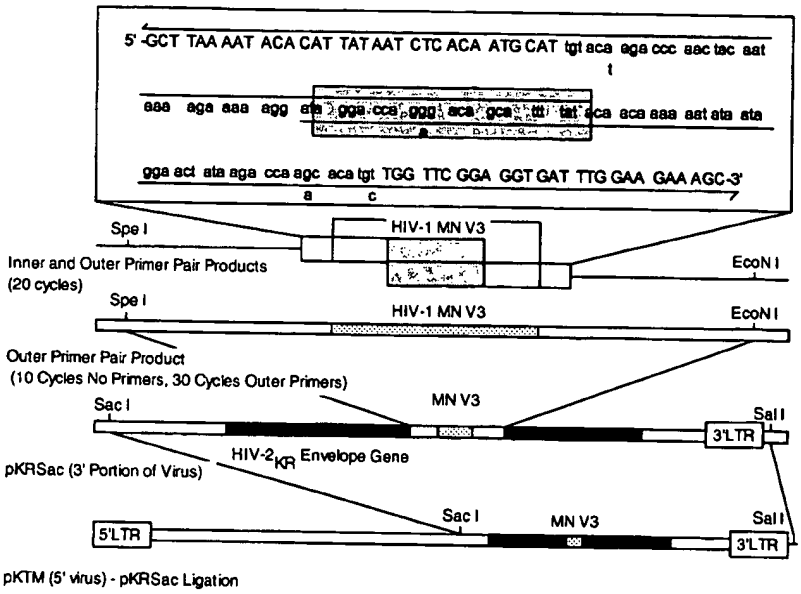

FIG. 1. Construction of HIV-2 and SIV V3 chimeric proviruses. HIV-2_{KR} and SIV_{239} HIV-1 V3 chimera construction is detailed in Materials and Methods. Shown are the sequences of overlapping primers (box at top) used to create a synthetic HIV-1_{MN} V3 coding region (lowercase bases), as well as regions of HIV-2_{KR} envelope primed (uppercase bases). The PCR products were then annealed (bars immediately below boxed area), and internal *Spe*I and *Eco*NI sites were used after amplification with the outer primers (next level down) to insert this fragment into pRTsac (next level, with fragment in light color and the MN V3 region shaded, with surrounding KR sequences in black). The *Sac*I-*Sal*I fragment of the chimeric 3' proviral plasmid was then ligated to the 5' portion of the provirus from plasmid pKTM digested with *Sac*I and used for transfection. SIV chimeras were created in an essentially identical fashion (see Materials and Methods).

SIV). Virus production was then monitored by a p26 antigen capture enzyme immunoassay at the times indicated (see Fig. 2). Wild-type HIV-2_{KR} displayed a rise in antigen production within 1 week following infection. Significant replication of the chimeric KR-MNV3 virus was also evident by p26 production after 2 to 3 weeks in culture, persisting until >7 weeks after transfection. In contrast, no replication of SIV-MNV3 virus was detected upon culture, though the initial amount of p26 produced after transfection of COS.1 cells was comparable (not shown). Syncytium formation was also evident in HIV-2_{KR}- and KR-MNV3-infected cultures (not shown). For subsequent experiments, concentrated stocks of HIV-2_{KR} and KR-MNV3 viruses were prepared by infecting large-scale Molt 4/8 cell cultures with filtered (0.2 μm) supernatants from initial transfection experiments and concentrating of supernatants from large-scale cultures by ultracentrifugation (see Materials and Methods).

Expression of chimeric envelope protein. To verify that a chimeric HIV-2 envelope protein containing the HIV-1_{MN} V3 loop was produced, labeled lysates of acutely infected Molt 4/8 cells were analyzed by radioimmunoprecipitation (see Fig. 3). With serum from an HIV-2-infected macaque (HIV-2^+), a ~115-kDa band was precipitated from protein lysates from both KR- and KR-MNV3-infected Molt 4/8 cells (Fig. 3, lanes H and K), but no band corresponding to HIV-2 *env* was detected in lysates from Jurkat cells infected with HIV-1_{MN} (Fig. 3, lane B). When pooled sera from a group of nine HIV-1-infected patients (HIV-1^+) was used for immunoprecipitation, a ~120-kDa band corresponding to *env* was precipitated from lysates of HIV-1_{MN}-infected cells (Fig. 3, lane A), and a ~115-kDa band was detected in cells infected by KR-MNV3 (Fig. 3, lane I), but sera to HIV-1 failed to detect *env* in lysates of cells infected with parental HIV-2_{KR} virus (Fig. 3, lane G: cross-reactive bands for *gag-pol* precursors were seen but are not shown).

Neutralization of KR-MNV3. We next examined the ability of a panel of HIV-1-specific antisera to neutralize KR-MNV3. Each had previously been shown to neutralize wild-type HIV-1_{MN}. Sera G18-9 and G19-9 (gift of Thomas Palker) were obtained from goats immunized with an MN V3 loop peptide coupled to the T-helper epitope Sp10. The sera designated GP06 and GP09 were raised in guinea pigs immunized with a cocktail of octameric V3 peptides, which included MN V3 p200 (gift of United Biomedical Inc.). Serum from a stage III HIV-1-seropositive individual was also used.

Table 1 shows the neutralizing activity of each polyclonal serum against HIV-2_{KR}, KR-MNV3, and HIV-1_{MN}, expressed as the reciprocal geometric mean titer, with a 100× $TCID_{50}$ inoculum (see Materials and Methods). None of the sera tested displayed detectable neutralization of HIV-2_{KR}. In contrast, HIV-1_{MN} was neutralized by every HIV-1-specific serum tested, with G19-9 being the most effective and G18-9 having only a modest neutralizing effect. The KR-MNV3 chimera was susceptible to neutralization by all HIV-1-specific antisera, and titers against KR-MNV3 were higher than those against HIV-1_{MN} for all but one member of the antiserum panel. These values ranged from 64-fold-greater neutralizing effect on KR-MNV3 than on MN for the GP16 antiserum to 16-fold-greater neutralization for G19-9 antiserum. Conversely, GP06 antiserum, which had a significant neutralizing effect on MN, was not able to neutralize KR-MNV3.

Cell tropism of KR-MNV3. The V3 loop of HIV-1 has been implicated in viral tropism, including entry into monocyte-macrophages, as well as replication characteristics in a variety of lymphocytoid and monocytoid cell lines (12, 30, 35). To investigate whether substitution of the HIV-1_{MN} V3 loop altered the pattern of replication of the recombinant KR-MNV3, we compared the infectivity of KR-MNV3 and HIV-2_{KR} on a variety of cell lines (see Table 2). Viral p26 production by KR-MNV3 and HIV-2_{KR} was assessed 18 days after infection

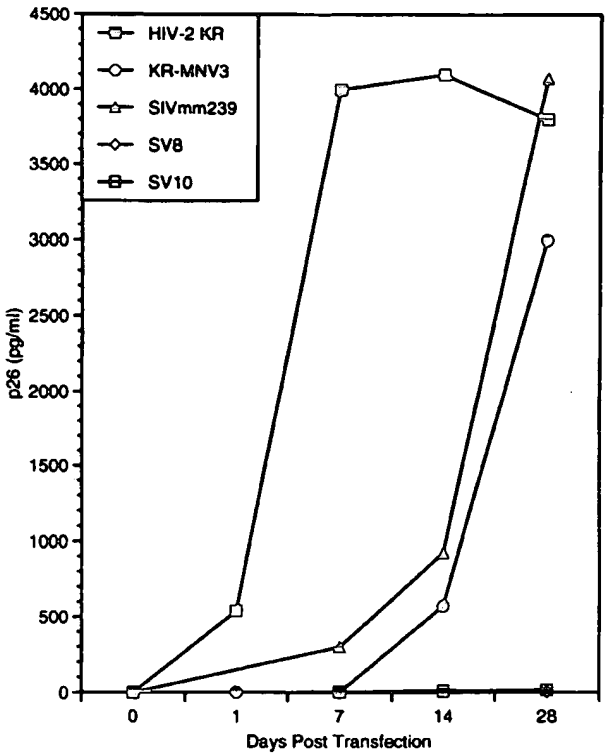

FIG. 2. Kinetics of p26 production by wild-type and chimeric viruses after transfection. Approximately 5 μg of the ligation mixture of 5′ and 3′ plasmids was used to transfect susceptible Molt 4/8 lymphoblastoid cells (SIV viruses) or to transfect COS.1 cells followed by cocultivation with Molt 4/8 cells (HIV-2 viruses). Cells were washed and placed in culture after transfection (see Materials and Methods) and/or after cocultivation for 48 h with COS.1 cells, and the supernatant was sampled at least weekly for 1 month. Shown are results of transfection with wild-type HIV-2 pKTM-pRTsac ligation (KR), chimeric HIV-2 pKTM-pRT-MN V3 ligation (KR-MNV3), wild-type SIV_{mm239} p239SPE and p239SPSP ligation (SIVwt), and two separate clones obtained from ligation of p239SPE and p229SPSP-MN V3 (SV8 and SV10, respectively). Note the prompt rise in antigen production by HIV-2_{KR}-transfected cultures, followed by a plateau and eventual tapering (cultures refed with fresh cells as well as medium to maintain viability), in contrast to the delayed production of p26 after transfection with KR-MNV3 and no evidence of productive infection after transfection with SIV chimeras.

of T-cell lines Molt 3, SupT1, H9, Molt 4/8, Jurkat, MT2, and MT4 and the monocytoid cell line U937 at an MOI of 0.01 $TCID_{50}$/cell. By 18 days postinfection, parental KR had established infection in each cell line tested, while KR-MNV3 showed reduced growth in a number of the cell lines tested, with very low production of p26 in SupT1, H9, Jurkat, and U937 cells. By 36 days postinfection, KR-MNV3 had established infection in all cell lines tested except the monocytoid cell line U937, in which no infection was observed. As both HIV-2_{KR} and HIV-1_{MN} are capable of monocyte infection, KR-MNV3 represents the substitution of one monocyte-permissive V3 loop for another. Thus, the inability of the chimeric virus to replicate in U937 cells was not predicted.

The ability of the chimeric virus to infect primary human PBMC was also tested. Purified PHA-stimulated PBMC were infected at an MOI of 0.1 $TCID_{50}$/cell. At various times, samples were taken for p26 determination. The growth kinetics of KR and KR-MNV3 are shown in Fig. 4. The data indicate that KR-MNV3 is able to productively infect human PBMC, although p26 production was delayed compared with that of parental KR virus.

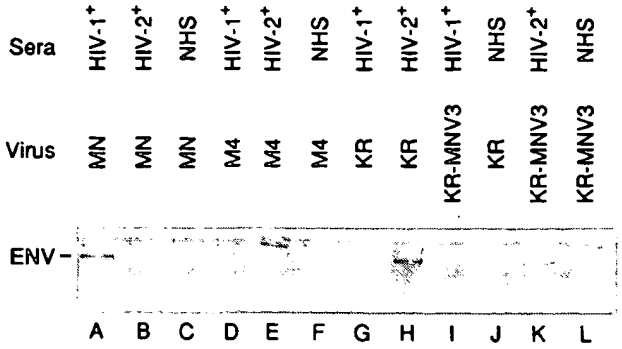

FIG. 3. Radioimmunoprecipitation of chimeric envelope proteins. Radiolabeled cell lysates (see Materials and Methods) from cells infected with HIV-1_{MN} (lanes A to C), HIV-2_{KR} (lanes G, H, and J), or HIV-$2_{KR\text{-}MNV3}$ (lanes I, K, and L) and uninfected control cultures (lanes D, E, and F) were immunoprecipitated with pooled sera from HIV-1-seropositive individuals (lanes A, D, G, and I), normal human serum (lanes C, F, and J), and serum from a pigtailed macaque infected with HIV-2_{KR} (lanes B, E, H, and K). Normal human serum does not recognize envelope from cells infected with either HIV-1_{MN} (C), HIV-2_{KR} (J), or HIV-$2_{KR\text{-}MNV3}$ (L). HIV-1-positive pooled serum precipitates the expected-size band from HIV-1_{MN}-infected cells (A) and from HIV-$2_{KR\text{-}MNV3}$-infected cell lysates (I), but not from HIV-2_{KR}-infected cell lysates (G). Serum from an HIV-2_{KR}-infected macaque precipitated envelope bands from both HIV-2_{KR}- and HIV-$2_{KR\text{-}MNV3}$-infected cell lysates (H and K) but not from lysates of HIV-1_{MN}-infected cells (B). (Cross-reactivity of both HIV-1- and HIV-2-seropositive sera to *pol* and *gag* was seen [not shown].)

Sequence of the infectious chimeric virus. Because a long lag was observed between transfection of the recombinant proviral clone of the chimeric virus and productive infection, it is possible that a compensatory mutation(s) might have been required to allow generation of infectious progeny capable of spreading in the culture, though this was made less likely by the observation that virus preparations from passaged virus did not display accelerated replication kinetics (not shown). To further investigate this possibility, genomic DNA from Molt 4/8 cells infected by KR-MNV3 was prepared, and the V3 loop and flanking sequences were amplified by PCR. Subsequently, the pool of amplified fragments was cloned into a T/A cloning vector, and 10 of the resulting clones were selected for sequencing. No consistent amino acid change was observed in the V3 loop or flanking sequences. Some individual clones did show amino acid changes, but since these changes were not present in at least two clones, these were attributed to random changes or errors occurring during PCR amplification.

TABLE 1. Neutralization of parental and chimeric viruses by HIV-1-specific antisera[a]

Serum[b]	Titer		
	HIV-2_{KR}	HIV-1_{MN}	HIV-$2_{KR\text{-}MNV3}$
G19-9	4	512	8,192
G18-9	4	16	512
GP06	4	64	4
GP16	4	64	4,096
RBC	4	64	64
NGPS	4	4	4

[a] Neutralizations were performed in quadruplicate on Molt 4/8 cells as described in the text. Values shown represent the reciprocal geometric mean titers which produced at least a 90% reduction in syncytia in the culture.

[b] G19-9 and G18-9, goat monospecific polyclonal antisera to the HIV-1_{MN} V3 loop (T. Palker); GP06 and GP16, guinea pig polyclonal antisera to V3-MAP octameric peptide mixtures (C. Y. Wang); RBC, human serum from a healthy HIV-1-seropositive patient; and NGPS, normal guinea pig serum.

TABLE 2. Growth of HIV-$2_{KR-MNV3}$ in cell lines and primary cells[a]

Cells[b]	p26 production (optical density) at day postinfection:					
	4	7	11	18	25	36
Molt 3	0	0	0	3,057	>4,200	>4,200
SupT1	0	0	0	176	>4,200	>4,200
H9	0	0	0	349	240	>4,200
Molt 4/8	0	0	0	1,028	>4,200	>4,200
Jurkat	0	0	0	307	>4,200	>4,200
U937	0	0	0	113	167	85
MT2	0	0	0	1,251	848	>4,200
MT4	0	0	0	1,528	196	>4,200
PBMC	0	2,945	17,224	ND[c]	ND	ND

[a] Virus pools derived from transfection and expanded in Molt 4/8 cells (see Fig. 2 and Materials and Methods) were used to infect a variety of lymphoid cell lines, at an inoculum corresponding to 0.01 (for cell lines) or 0.1 (for PBMC) $TCID_{50}$/cell as determined by prior titration on Molt 4/8 cells. Shown are optical densities representing p26 production in cultures infected with HIV-$2_{KR-MNV3}$ after up to 7 weeks in culture (parental HIV-2_{KR} p26 production was offscale in all cell lines by the first week after infection [not shown]). The chimeric KR-MNV3 virus appeared to be capable of slower but significant growth in all lines tested except for U937 and showed the greatest lag in SupT1 and MT4 lymphoblastoid cells (maximum p26 production did not occur until day 36).

[b] Molt 3, SupT1, H9, Molt 4/8, and Jurkat are uninfected $CD4^+$ lymphoblastic cell lines. MT2 and MT4 are HTLV-I-transformed $CD4^+$ lymphoblastic cell lines. U937 is a myelomonocytic line expressing very low levels of surface CD4. PBMC are PHA-P- and IL-2-stimulated human mononuclear cells from a normal volunteer donor separated by Ficoll-Hypaque centrifugation.

[c] ND, not done.

DISCUSSION

A chimeric HIV-2_{KR} virus containing the MN V3 loop was constructed and found to be infectious and capable of replicating in a wide variety of T-cell lines and human PBMC. A virtually identical insertion of the HIV-1 V3 loop into the SIV_{mm239} envelope led to a biologically inactive chimeric virus, as replication of transfected provirus could not be detected in CEMX174 cells or C8166 cells, both of which are highly permissive for SIV replication. Similar negative results have been reported previously (15). The growth kinetics of the chimeric HIV-2_{KR} clone were affected by the substitution of the HIV-1 V3 loop in a number of cell lines, as the chimeric virus took considerably longer to establish infection in SupT1, H9, and Jurkat cells. Furthermore, the KR-MNV3 chimeric virus was unable to infect the monocytoid line U937 (see Table 2), while both wild-type parental viruses (HIV-2_{KR} and HIV-1_{MN}) were capable of replication in this cell line, as well as primary monocyte-macrophages (17) (not shown).

These results suggest that HIV-2 tolerates a high degree of variability in the V3 region, in contrast to SIV (perhaps reflected in the overall variability of this region in available sequences). However, the region homologous with the HIV-1 V3 has been shown to be important for SIV cell tropism as well, and some variability appears to be tolerated (11, 14, 15). The data demonstrate changes in the tropism and growth rate of the chimeric HIV-2 virus, suggesting that for HIV-2, as well as HIV-1, the V3 region is important for viral entry and establishment and maintenance of infection in a number of different cell types.

It is unlikely that the compatibility of HIV-2_{KR} with the HIV-1_{MN} PND is due to inadvertent introduction of distant envelope mutations or selection of such compensatory mutations in culture. Note that only infrequent, minor V3 variants were present in viral genomes sequenced in expanded cultures. Also, note that the phenotype of the expanded chimeric virus was stable (Table 2), as the KR-MNV3 virus consistently exhibited delayed replication in diverse cell types after passage and expansion in Molt 4/8 cells, making distant compensatory mutations in *env* or other genes a less likely possibility.

Although the tropism of KR-MNV3 is altered, the V3 loop region must take on a conformation which is similar to that of its native form, as a number of sera which neutralize HIV-1_{MN} were found to display potent neutralization of the chimeric virus. The neutralizing titers of most monospecific polyclonal antibodies were much higher against the chimeric virus than against HIV-1_{MN}. Conversely, one HIV-1 V3-specific serum which was capable of neutralizing HIV-1_{MN} was not capable of neutralizing the chimeric virus. Increased sensitivity of chimeric viruses bearing the MN V3 loop to neutralizing sera directed against this epitope is not without precedent, as a chimeric HIV-1_{HXB2} bearing the MN V3 loop was found to be much more neutralizable than HIV-1_{MN} itself (29), and chimerics of human rhinovirus type 14 expressing V3 loop epitopes were also found to be exquisitely sensitive to the neutralizing effects of HIV-1 V3-specific antisera (31), as noted for this HIV-1/HIV-2 chimera. Several possibilities might account for these observations. First, the chimeric V3 loop might be more exposed on the HIV-2 envelope protein than on the native HIV-1 envelope. Alternatively, the chimeric envelope might be more susceptible to the action of bound antibody than native HIV-1 envelope, or the chimeric V3 region may be presented in a conformation more favorable for functional antibody binding. This result also suggests that factors which influence the overall conformation of the HIV-1 V3 loop are largely similar in the context of HIV-1 and HIV-2 envelope proteins.

It should be of considerable interest to determine if HIV-$2_{KR-MNV3}$ (or other viable HIV-2/HIV-1 V3 chimeras) are infectious in macaques and if the behavior of this virus in vivo makes it useful as a challenge virus in V3 peptide-immunized animals. The use of HIV-2/HIV-1 V3 chimeras may offer a less expensive and useful alternative to the SHIV/macaque and HIV-1/chimpanzee models for the evaluation of vaccine strategies directed against the PND of HIV-1.

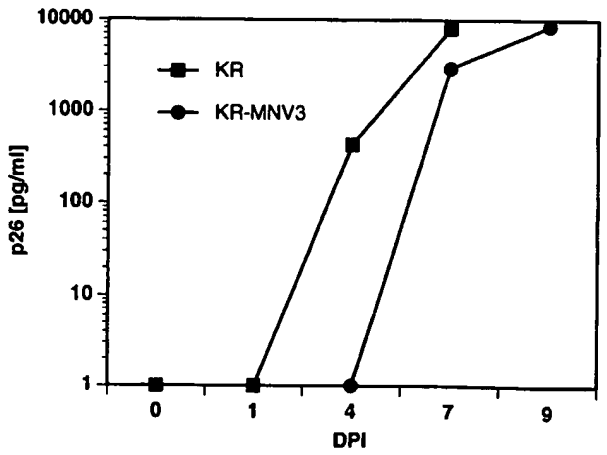

FIG. 4. Replication of HIV-2_{KR} and HIV-$2_{KR-MNV3}$ in primary cells. Mononuclear cells were obtained from a normal volunteer donor by Ficoll-Hypaque centrifugation. Cells were stimulated with PHA-P (5 μg/ml) for 48 h and IL-2 (200 U/ml) for 24 h before infection. PBMC (10^7) were infected with HIV-2_{KR} and HIV-$2_{KR-MNV3}$ at an MOI of 0.1 $TCID_{50}$/cell, as determined by prior titration on Molt 4/8 cells. The supernatant was sampled on the first day after infection and at days 4, 9, and 11, with replacement of the culture medium (RPMI 1640 with 10% fetal calf serum and 200 U of IL-2 per ml). Antigen production by HIV-2_{KR} was detectable within 4 days of infection, whereas HIV-$2_{KR-MNV3}$ p26 production was not detectable until 7 days after infection, while maximal p26 production was comparable.

ACKNOWLEDGMENTS

Support for this project was provided by the National Institutes of Allergy and Infectious Disease through RO1 AI29889 (In Vivo and In Vitro Parameters of HIV-2 Pathogenicity) and National Collaborative Vaccine Development Groups program project grant (Strategies for HIV Vaccine Development) U01AI30238. Additional support was provided through the Centers for AIDS Research P30 AI36214-01, UCSD CFAR Molecular Biology Core and Virology Core.

We thank Gunter Kraus for providing the initial starting material for HIV-2 chimeric viruses and David Kang, Patricia Badel, Kristine Menihan, and Silvestre Ramos for technical assistance.

REFERENCES

1. **Agy, M. B., L. R. Frumkin, L. Corey, R. W. Coombs, S. M. Wolinsky, J. Koehler, W. R. Morton, and M. G. Katze.** 1992. Infection of Macaca nemestrina by human immunodeficiency virus type-1. Science **257**:103–106.
2. **Arthur, L. O., J. W. Bess, Jr., D. J. Waters, S. W. Pyle, J. C. Kelliher, P. L. Nara, K. Krohn, W. G. Robey, A. J. Langlois, R. C. Gallo, and P. J. Fischinger.** 1989. Challenge of chimpanzees (*Pan troglodytes*) immunized with human immunodeficiency virus envelope glycoprotein gp120. J. Virol. **63**: 5046–5053.
3. **Barnett, S. W., M. Quiroga, A. Werner, D. Dina, and J. A. Levy.** 1993. Distinguishing features of an infectious molecular clone of the highly divergent and noncytopathic human immunodeficiency virus type 2 UC1 strain. J. Virol. **67**:1006–1014.
4. **Bjorling, E., F. Chiodi, G. Utter, and E. Norrby.** 1994. Two neutralizing domains in the V3 region in the envelope glycoprotein gp125 of HIV type 2. J. Immunol. **152**:1952–1959.
5. **Castro, B. A., M. Nepomuceno, N. W. Lerche, J. W. Eichberg, and J. A. Levy.** 1991. Persistent infection of baboons and rhesus monkeys with different strains of HIV-2. Virology **184**:219–226.
6. **Emini, E. A., W. A. Schleif, J. H. Nunberg, A. J. Conley, Y. Eda, S. Tokiyoshi, S. D. Putney, S. Matsushita, K. E. Cobb, C. M. Jett, et al.** 1992. Prevention of HIV-1 infection in chimpanzees by gp120 V3 domain-specific monoclonal antibody. Nature (London) **355**:728–730.
7. **Franchini, G., P. Markham, E. Gard, K. Fargnoli, S. Keubaruwa, L. Jagodzinski, M. Robert-Guroff, P. Lusso, G. Ford, F. Wong-Staal, and R. C. Gallo.** 1990. Persistent infection of rhesus macaques with a molecular clone of human immunodeficiency virus type 2: evidence of minimal genetic drift and low pathogenetic effects. J. Virol. **64**:4462–4467.
8. **Frumkin, L. R., M. B. Agy, R. W. Coombs, L. Panther, W. R. Morton, J. Koehler, M. J. Florey, J. Dragavon, A. Schmidt, M. G. Katze, et al.** 1993. Acute infection of Macaca nemestrina by human immunodeficiency virus type 1. Virology **195**:422–431.
9. **Fultz, P. N.** 1993. Nonhuman primate models for AIDS. Clin. Infect. Dis. **1**:S230–S235.
10. **Gorny, M. K., A. J. Conley, S. Karwowska, A. Buchbinder, J. Y. Xu, E. A. Emini, S. Koenig, and S. Zolla-Pazner.** 1992. Neutralization of diverse human immunodeficiency virus type 1 variants by an anti-V3 human monoclonal antibody. J. Virol. **66**:7538–7542.
11. **Hirsch, V. M., J. E. Martin, G. Dapolito, W. R. Elkins, W. T. London, S. Goldstein, and P. R. Johnson.** 1994. Spontaneous substitutions in the vicinity of the V3 analog affect cell tropism and pathogenicity of simian immunodeficiency virus. J. Virol. **68**:2649–2661.
12. **Hwang, S. S., T. J. Boyle, H. K. Lyerly, and B. R. Cullen.** 1991. Identification of the envelope V3 loop as the primary determinant of cell tropism in HIV-1. Science **253**:71–74.
13. **Javaherian, K., A. J. Langlois, S. Schmidt, M. Kaufmann, N. Cates, J. P. Langedijk, R. H. Meloen, R. C. Desrosiers, D. P. Burns, D. P. Bolognesi, et al.** 1992. The principal neutralization determinant of simian immunodeficiency virus differs from that of human immunodeficiency virus type 1. Proc. Natl. Acad. Sci. USA **89**:1418–1422.
14. **Kirchhoff, F., K. Mori, and R. C. Desrosiers.** 1994. The "V3" domain is a determinant of simian immunodeficiency virus cell tropism. J. Virol. **68**: 3682–3692.
15. **Kirchhoff, F., H. G. Morrison, M. G. Murray, P. Rennert, and R. C. Desrosiers.** 1994. SIVmac expressing hybrid envelope proteins containing HIV-1 V3 and/or C4 sequences is not competent for replication. AIDS Res. Hum. Retroviruses **10**:309–313.
16. **Koch, J. A., and R. M. Ruprecht.** 1992. Animal models for anti-AIDS therapy. Antiviral Res. **19**:81–109.
17. **Kraus, G., R. Talbot, M. Leavitt, L. Luznick, A. Schmidt, P. Badel, C. Bartz, W. Morton, F. Wong-Staal, and D. Looney.** Characterization of a novel molecular clone of HIV-2 infectious for *Macaca nemestrina*. Submitted for publication.
18. **Letvin, N. L.** 1992. Nonhuman primate models for HIV vaccine development. Immunodefic. Rev. **3**:247–260.
19. **Li, J., C. I. Lord, W. Haseltine, N. L. Letvin, and J. Sodroski.** 1992. Infection of cynomolgus monkeys with a chimeric HIV-1/SIVmac virus that expresses the HIV-1 envelope glycoproteins. J. Acquired Immune Defic. Syndr. **5**:639–646.
20. **Lusso, P., P. D. Markham, A. Ranki, P. Earl, B. Moss, F. Dorner, R. C. Gallo, and K. J. Krohn.** 1988. Cell-mediated immune response toward viral envelope and core antigens in gibbon apes (Hylobates lar) chronically infected with human immunodeficiency virus-1. J. Immunol. **141**:2467–2473.
21. **McClure, J., N. Haigwood, W. Morton, and S.-L. Hu.** Submitted for publication.
22. **Meyers, G., B. Korber, G. Pavlakis, and J. Berzofsky (ed.).** 1994. Human retroviruses and AIDS: Los Alamos AIDS database. Los Alamos National Laboratory, Los Alamos, N.Mex.
23. **Otten, R. A., B. G. Brown, M. Simon, L. D. Lupo, B. S. Parekh, M. D. Lairmore, C. A. Schable, G. Schochetman, and M. A. Rayfield.** 1994. Differential replication and pathogenic effects of HIV-1 and HIV-2 in Macaca nemestrina. AIDS **8**:297–306.
24. **Palker, T. J., M. E. Clark, A. J. Langlois, T. J. Matthews, K. J. Weinhold, R. R. Randall, D. P. Bolognesi, and B. F. Haynes.** 1988. Type-specific neutralization of the human immunodeficiency virus with antibodies to env-encoded synthetic peptides. Proc. Natl. Acad. Sci. USA **85**:1932–1936.
25. **Palker, T. J., T. J. Matthews, A. Langlois, M. E. Tanner, M. E. Martin, R. M. Scearce, J. E. Kim, J. A. Berzofsky, D. P. Bolognesi, and B. F. Haynes.** 1989. Polyvalent human immunodeficiency virus synthetic immunogen comprised of envelope gp120 T helper cell sites and B cell neutralization epitopes. J. Immunol. **142**:3612–3619.
26. **Putkonen, P., R. Thorstensson, J. Albert, K. Hild, E. Norrby, P. Biberfeld, and G. Biberfeld.** 1990. Infection of cynomolgus monkeys with HIV-2 protects against pathogenic consequences of a subsequent simian immunodeficiency virus infection. AIDS **4**:783–789.
27. **Reed, L. J., and H. Muench.** 1938. A simple method of estimating 50% endpoints. Am. J. Hyg. **27**:493–497.
28. **Regier, D. A., and R. C. Desrosiers.** 1990. The complete nucleotide sequence of a pathogenic molecular clone of simian immunodeficiency virus. AIDS Res. Hum. Retroviruses **6**:1221–1231.
29. **Robert-Guroff, M., A. Louie, M. Myagkikh, F. Michaels, M. P. Kieny, M. E. White-Scharf, B. Potts, D. Grogg, and M. S. Reitz, Jr.** 1994. Alteration of V3 loop context within the envelope of human immunodeficiency virus type 1 enhances neutralization. J. Virol. **68**:3459–3466.
30. **Shioda, T., J. A. Levy, and C. Cheng-Mayer.** 1992. Small amino acid changes in the V3 hypervariable region of gp120 can affect the T-cell-line and macrophage tropism of human immunodeficiency virus type 1. Proc. Natl. Acad. Sci. USA **89**:9434–9438.
31. **Smith, A. D., D. A. Resnick, A. Zhang, S. C. Geisler, E. Arnold, and G. F. Arnold.** 1994. Use of random systematic mutagenesis to generate viable human rhinovirus 14 chimeras displaying human immunodeficiency virus type 1 V3 loop sequences. J. Virol. **68**:575–579.
32. **Talbott, R., G. Kraus, D. J. Looney, and F. Wong-Staal.** 1993. Mapping the determinants for infectivity, replication efficiency and cytopathicity of HIV-2. Proc. Natl. Acad. Sci. USA **90**:4226–4230.
33. **Wang, C. Y., D. J. Looney, M. L. Li, A. M. Walfield, J. Ye, B. Hosein, J. P. Tam, and F. Wong-Staal.** 1991. Long-term high-titer neutralizing activity induced by octameric synthetic HIV-1 antigen. Science **254**:285–288.
34. **Watkins, B. A., A. E. Davis, F. Cocchi, and M. S. Reitz, Jr.** 1993. A rapid method for site-specific mutagenesis using larger plasmids as templates. Biotechniques **15**:700–704.
35. **Westervelt, P., H. E. Gendelman, and L. Ratner.** 1991. Identification of a determinant within the human immunodeficiency virus 1 surface envelope glycoprotein critical for productive infection of primary monocytes. Proc. Natl. Acad. Sci. USA **88**:3097–3101.
36. **Whitescharf, M. E., B. J. Potts, L. M. Smith, K. A. Sokolowski, J. R. Rusche, and S. Silver.** 1993. Broadly neutralizing monoclonal antibodies to the V3-region of HIV-1 can be elicited by peptide immunization. Virology **192**:197–206.

09/764,918

```
Your SELECT statement is:
   s albumin? and cysteine(w)loop

          Items   File
          -----   ----
              1   149: TGG Health&Wellness DB(SM)_1976-2002/Nov W4

   1 file has one or more items; file list includes 27 files.
 Set  Items  Description
      ---  -----  -----------
?s albumin and cysteine(w)loop
           6226  ALBUMIN
           1636  CYSTEINE
           5314  LOOP
              5  CYSTEINE(W)LOOP
      S1       1  ALBUMIN AND CYSTEINE(W)LOOP
26     5: Biosis Previews(R)_1969-2002/Dec W1
             32    34: SciSearch(R) Cited Ref Sci_1990-2002/Dec W2
              1    35: Dissertation Abs Online_1861-2002/Nov
              7    71: ELSEVIER BIOBASE_1994-2002/Dec W1
             25    73: EMBASE_1974-2002/Dec W1
              2    94: JICST-EPlus_1985-2002/Oct W1
              1   135: NewsRx Weekly Reports_1995-2002/Dec W1
              6   144: Pascal_1973-2002/Dec W2
             12   149: TGG Health&Wellness DB(SM)_1976-2002/Nov W4
             22   155: MEDLINE(R)_1966-2002/Nov W3
              5   156: ToxFile_1965-2002/Nov W3
              1   159: Cancerlit_1975-2002/Oct
              1   162: CAB Health_1983-2002/Oct
              1   370: Science_1996-1999/Jul W3
              5   399: CA SEARCH(R)_1967-2002/UD=13724
              2   434: SciSearch(R) Cited Ref Sci_1974-1989/Dec
              9   442: AMA  Journals_1982-2002/Dec B3
              2   444: New England Journal of Med._1985-2002/Dec W2

SYSTEM:OS  - DIALOG OneSearch
  File   5:Biosis Previews(R)  1969-2002/Dec W1
         (c) 2002 BIOSIS
*File   5: Alert feature enhanced for multiple files, duplicates
removal, customized scheduling. See HELP ALERT.
  File  34:SciSearch(R) Cited Ref Sci  1990-2002/Dec W2
         (c) 2002 Inst for Sci Info
*File  34: Alert feature enhanced for multiple files, duplicates
removal, customized scheduling. See HELP ALERT.
  File  73:EMBASE  1974-2002/Dec W1
         (c) 2002 Elsevier Science B.V.
*File  73: Alert feature enhanced for multiple files, duplicates
removal, customized scheduling. See HELP ALERT.
  File 155:MEDLINE(R)  1966-2002/Nov W3
*File 155: For updating information please see Help News155. Alert
feature enhanced with customized scheduling. See HELP ALERT.
Set  Items  Description
      ---  -----  -----------
?s human(w)serum(w)albumin
Processing
         18775262  HUMAN
          1694602  SERUM
           297500  ALBUMIN
      S1    26108  HUMAN(W)SERUM(W)ALBUMIN
?s hsa
      S2    12534  HSA
?s (s1 or s2) and loop
            26108  S1
            12534  S2
           220802  LOOP
      S3      113  (S1 OR S2) AND LOOP
?s s3 and (chimeric or heterolo?)
              113  S3
            73025  CHIMERIC
```

```
          119138  HETEROLO?
      S4       2  S3 AND (CHIMERIC OR HETEROLO?)
?rd
...completed examining records
      S5       2  RD (unique items)
```

Set	Items	Description
S1	26108	HUMAN(W)SERUM(W)ALBUMIN
S2	12534	HSA
S3	113	(S1 OR S2) AND LOOP
S4	2	S3 AND (CHIMERIC OR HETEROLO?)
S5	2	RD (unique items)
S6	711	(S1 OR S2) AND CYS?
S7	9	S6 AND (CHIM? OR HETERO?)
S8	7	RD (unique items)